RSC Advances

PAPER

View Article Online
View Journal | View Issue

Cite this: *RSC Adv.*, 2024, **14**, 37633

Advanced functional Cu–Cr–Co-NPs@gelatin (GLN)-hydroxyethyl cellulose (HEC) nanocomposites with antimicrobial and anticancer activities

Mohamed S. Hasanin, [ab] Mohammad Reza Saeb, [c] Mostafa A. Abdel-Maksou,[d] Mohamed A. El-Tayeb,[d] Bushra Hafeez Kiani [e] and Amr H. Hashem [*f]

An advanced hybrid nanocomposite based on different metals (copper, cobalt, and chromium) decorated with sustainable polysaccharides (gelatin, GLN, and hydroxyethyl cellulose, HEC) was developed. The composite reflects several advantages including a controlled particle size, particle size distribution, along with promising antimicrobial and anticancer activities. Topographical and elemental analyses were carried out using field-emission scanning electron microscopy (FE-SEM), high-resolution transmission electron microscopy (HR-TEM), and energy dispersive X-ray analysis (EDX), demonstrating the formation of trimetallic nanoparticles (NPs) possessing domain sizes of 169 nm and 102 nm assigned to the free nanocomposite (Fcomp) and loaded nanocomposite (Lcomp), respectively. Moreover, antimicrobial and anticancer activities were evaluated for so-called Cu–Cr–Co-NPs@GLN-HEC nanocomposites. Antimicrobial results revealed that the synthesized Cu–Cr–Co-NPs@GLN-HEC nanocomposite exhibited outstanding antibacterial activity toward *S. typhimurium*, *P. aeruginosa*, *S. aureus* and *S. mutans* with MICs of 125, 62.5, 125 and 7.81 μg mL^{-1}, respectively. Likewise, the synthesized Cu–Cr–Co-NPs@GLN-HEC nanocomposite showed promising antifungal activity against *C. albicans* and *C. neoformans*, with MICs of 31.25 and 15.62 μg mL^{-1}, respectively. Furthermore, the cytotoxicity of Cu–Cr–Co-NPs@GLN-HEC was assessed toward the Wi38 normal cell line, labeled for half-maximal inhibitory concentration (IC_{50}) of 170.8 μg mL^{-1}. Furthermore, the Cu–Cr–Co-NPs@GLN-HEC nanocomposite exhibited strong anticancer activity toward the MCF7 cancerous cell line with IC_{50} = 30.4 μg mL^{-1}. In conclusion, the synthesized Cu–Cr–Co-NPs@GLN-HEC nanocomposite has promising antibacterial, antifungal and anticancer activities, which can be used in the medical field after excessive experiments *in vivo*.

Received 28th August 2024
Accepted 25th September 2024

DOI: 10.1039/d4ra06216g

rsc.li/rsc-advances

Introduction

Materials science has been long practised, but it continues to grow dynamically through multidisciplinary and interdisciplinary channels.[1] Biomedical materials, or also known as biomaterials, are a class of advanced materials with diverse types, which are growing in an accelerated speed, particulalrly because of the need for controlling and minimizing side effects and resistance to discovered drugs.[2,3] In a closer look, microbial infections resulting from the invasion of microorganisms, including bacteria, viruses, fungi, and parasites are attacking and accumulating into different spots of the human body. The severity of these illnesses can vary, and they can greatly affect human health.[4] Bacterial infections arise when pathogenic bacteria infiltrate the body and proliferate, resulting in diverse symptoms and consequences.[5,6] Fungal infections are caused by fungal organisms, which are living beings that exist in the environment.[7] The symptoms of microbial infections might differ based on the specific bacteria and the location of the infection. Typical symptoms comprise elevated body temperature, exhaustion, respiratory discomfort, gastrointestinal disturbance, skin eruption, and discomfort in the abdominal region.[8] The management of microbial infections typically entails the administration of antimicrobial agents, including antibiotics, antivirals, antifungals, or antiparasitics, depending on the nature of the infection.

[a]*Cellulose & Paper Department, National Research Centre, El-Buhouth St., Dokki, 12622, Egypt*

[b]*Department of Polymer and Biomaterials Science, West Pomeranian University of Technology in Szczecin, Al. Piastow 45, 70-311 Szczecin, Poland*

[c]*Department of Pharmaceutical Chemistry, Medical University of Gdańsk, J. Hallera 107, 80-416 Gdańsk, Poland*

[d]*Botany and Microbiology Department, College of Science, King Saud University, P. O. Box 2455, Riyadh 11451, Saudi Arabia. E-mail: mabdmaksoud@ksu.edu.sa; Mali5@ksu.edu.sa*

[e]*Department of Biology and Biotechnology, Worcester Polytechnic Institute, Worcester, Massachusetts, 01609, USA. E-mail: bushra.hafeez@iiu.edu.pk*

[f]*Botany and Microbiology Department, Faculty of Science, Al-Azhar University, Cairo 11884, Egypt. E-mail: amr.hosny86@azhar.edu.eg*

Antimicrobial resistance (AMR) is a worldwide issue concerning public health that pertains to the capacity of microorganisms, including bacteria, viruses, fungi, and parasites, to withstand the impact of antimicrobial medications.[9] Microorganisms can develop mechanisms that allow them to survive and reproduce despite exposure to antimicrobial medications, even while these treatments are being applied. As a result, the drug-resistant strains of previously treated microbes would be sustained.[10] Typically, a number of factors can contribute to the development and dissemination of antibiotic resistance, but mainly an inappropriate and excessive utilization of antimicrobial medications, in both human medicine and animal farming, poses the greatest impact on antibiotic resistance.[11] Moreover, the incorrect prescription methods, non-compliance with the whole course of antibiotics, and utilization of antibiotics in livestock to promote growth can be named. The use of antimicrobials creates a selection pressure that provides support for the survival and multiplication of resiliant bacteria.[11] Antimicrobial management has gained increasing awareness in recent years due to its significance in optimizing the use of antimicrobial medications and reducing the development of resistance.[12] This encompasses the promotion of suitable prescribing practices, the dissemination of knowledge to healthcare professionals and the general public regarding the responsible utilization of antimicrobials, and the execution of tactics to minimize the needless utilization of these medications.[9]

A complex and multifaceted health issue, cancer affects millions of people worldwide. From a closer look, cancer refers to a general term used to describe a group of diseases characterized by the unchecked growth and spread of abnormal cells throughout the body. Because they are abnormal cells, cancer cells can invade nearby tissues and organs, causing damage and interfering with normal body functions.[13,14] Reducing the impact of cancer requires early detection and prevention efforts. A healthy lifestyle (including regular exercise, eating a balanced diet, and abstaining from tobacco and excessive alcohol), protecting oneself from known carcinogens, getting vaccinated against infections that can cause cancer, and getting regular cancer screenings are all examples of preventive measures.[15,16] On the other hand, success in controlling and curing cancer depends on advancements in cancer diagnosis and therapy, which are nowadays of vital importance, particularly combination therapies improved the survival rates and thereby the quality of life has increased as per statistics collected from several cancer patients. Despite such attempts and progresses, there are still obstacles to overcome, which are social, economic, and also political to some extent, *e.g.*, discrepancies in outcomes of treatment of cancer as well as difficulties in transplantation of personalized data on treatments and clinical trials.[17,18]

There has been continued attempt to explore and apply noval materials possessing multiple biological functions in biomedical applications. Biopolymers are a group of materials known for their appropriate biomedical functions with minimal side effects. Gelatin, also known as gelatine, is a transparent, flavorless, and colorless food component that is often made from collagen extracted from animal tissues.[19] When dry, it is brittle; when wet, it becomes rubbery. After hydrolysis, it can also be referred to as hydrolyzed collagen. It is frequently employed as a GLNling agent in pharmaceutical, food, beverage, and cosmetic applications.[20] In addition, cellulose and its derivatives present excellent cytocompatibility and biodegradability.[21] Hydroxyethyl cellulose thickening and GLNling agent are made from cellulose and are extensively utilized in cleaning products, cosmetics, and other household goods.[22] In capsule formulations, hydroxyethyl and methyl cellulose are often combined with hydrophobic medicines to enhance the medications' breakdown in the gastrointestinal fluids. Accordingly, biopolymers have played a role in the formulation of bioactive materials to enhance their activity and reduce their side effects as well.

In addition to biopolymers and their derivatives, several metal nanoparticles have played a restricted role in antimicrobial activity and anti-cancer activity[23,24] such as silver nanoparticles (AgNPs),[25] gold nanoparticles (AuNPs),[26] zinc oxide nanoparticles (ZnONPs),[27] copper and copper oxide nanoparticles (CuNPs, Cu_2ONPs and CuONPs),[28,29] cobalt nanoparticles (CoNPs),[30] and chromium nanoparticles (CrNPs).[31] However, despite its promising features besides complicated formulation and optimization, a few has been reported about the hybridization of biopolymers and medical grade nanoparticles with complementary or synergistic effects. The formulation of trimetallic nanoparticles loaded in nanocomposite-based biologically compatible components is strongly recommended in the scientific community to cover a broad spectrum of biological activity applications. In this work, a novel formulation of trimetal nanoparticles based on copper, chromium and cobalt (Cu–Cr–Co-NPs) were loaded into the nanocomposite-based gelatin and hydroxyethyl cellulose. The formulate-free and loaded composites were investigated using physicochemical and topographical analysis in addition to the biological profile including antimicrobial activity assay, anticancer activity and cytotoxicity assays.

Materials and methods

Gelatin Bovine-B (GL) and hydroxyethyl cellulose (HEC) were obtained from Sigma Aldrich, USA. Chromium(III) acetate,

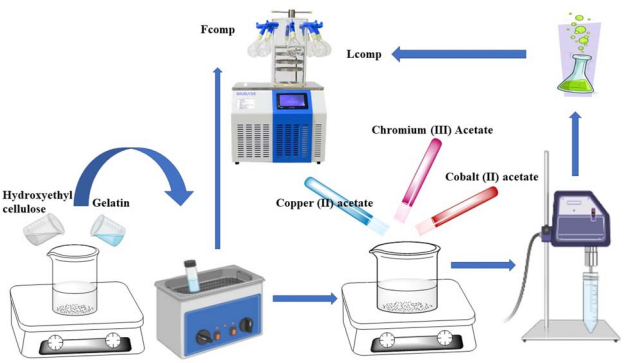

Scheme 1 Preparation of the nanocomposites.

cobalt(II) acetate, and copper(II) acetate were purchased from Sigma-Aldrich (Schnell Dorf, Germany).

Preparation of the nanocomposite

In this work, the template of the nanocomposite-based nanometal was prepared in two steps, as shown in Scheme 1. The first one involved the preparation of the free nanocomposite using gelatin solution (1% w/v) that was stirred for 2 h with hydroxyethyl cellulose solution (1% w/v) in equal volumes (100 mL). The collected homogenous solution was ultrasonicated in an ultrasonic water bath for 1 h at 70 °C and divided into equal volumes. One of these solutions was lyophilized and called free nanocomposite (Fcomp) and the other one was subject to loading with the trimetallic nanoparticles. The second step involved the loading of the trimetallic nanoparticles into the nanocomposite (Lcomp) *via* a green method. The above solution was stirred at 1500 rpm and copper acetate was added as 100 mg/100 mL of the above solution and allowed to dissolve. Chromium acetate and cobalt acetate were added as 50 mg mL^{-1} of the above solution individually. The solution was stirred for 2 h after the last addition and the temperature decreased to 40 °C and left for 2 h again. The collected solution was ultrasonicated for 15 min with an ultrasonic probe and ultrasonicated in an ultrasonic water bath for 3 h at 70 °C. Tannic acid was added in fixed amounts in both nanocomposites as 100 mg. The collected nanocomposite was washed several times with absolute methanol, then resuspended in deionized water and lyophilized and preserved in a refrigerator for further use.

Characterization

Characterization of the formulated nanocomposite was carried out for the free and loaded and neat materials as well. The physicochemical analysis included FTIR (Fourier transform infrared spectrophotometry) (model FT/IR-6100 type A), which was used to investigate the chemical functional groups of the SiNPs and βC-SiNPs nanoparticles. The spectra were recorded in the wavenumber range of 400–4000 cm^{-1}. XRD (X-ray diffraction) analysis was carried out in the 2θ (Bragg angle) range of 5–80° using a Bruker D8 Advance X-ray diffractometer (Germany), and DLS (dynamic laser scattering) measurement was carried out in triplicate, and the result was recorded as the average of three trials with standard division using a DLS instrument (Santa Barbara, CA, USA) to ascertain the average size in the following conditions: 23 °C, with the incident light being the 632.8 nm line of a HeNe laser at an angle of 13.9°. Topographical analysis included SEM-EDX analysis using an FE-SEM instrument (field emission scanning electron microscopy coupled with an energy dispersive X-ray spectrometer; Model Quanta 250 FEG (Field Emission Gun)) and HR-TEM (high-resolution transmission electron microscopy, JEM-2100, JEOL, Japan).

Antimicrobial activity

The antimicrobial activity of Cu–Cr–Co-NPs@GLN-HEC and GLN-HEC against *Salmonella typhimurium* ATCC 14028, *Pseudomonas aeruginosa* ATCC 27853, *Staphylococcus aureus* ATCC 25922, *Streptococcus mutans* ATCC 25175, *Candida albicans* ATCC 90028, and *C. neoformans* ATCC 14116 was evaluated using the agar-well diffusion technique. Minor modifications were made to the M51-A2 document of the Clinical Laboratory Standard Institute[32] when performing the agar diffusion test. Cu–Cr–Co-NPs@GLN-HEC and GLN-HEC, standard antibiotic (ampicillin/sulbactam)/standard antifungal (nystatin) were added to agar wells (8 mm) inoculated plates with bacterial and fungal strains individually at a concentration of 1000 μg mL^{-1}.

The diameter of the inhibition zone for all the treatments was measured. To determine minimum inhibitory concentration, Cu–Cr–Co-NPs@GLN-HEC was prepared in different concentrations ranging from 1000 to 3.9 μg mL^{-1} and then tested separately against selected bacterial and fungal strains.[33–35]

Cytotoxicity

The cytotoxicity of Cu–Cr–Co-NPs@GLN-HEC and GLN-HEC was determined using the MTT protocol[36] with minor modifications. The normal Wi38 and cancerous MCF7 cell lines were collected using American-type culture collection (ATCC). The cell quantity and the percentage of viable cell were determined by the following formulas.

$$\text{Viability\%} = \frac{\text{Test OD}}{\text{Control OD}} \times 100$$

$$\text{Inhibition\%} = 100 - \text{viability\%}$$

Moreove, the selectivity index (SI) was calculated according to the following formula, in which IC_{50} stands for the half-maximal inhibitory concentration.

$$\text{SI} = \frac{IC_{50} \text{ of a compound toward normal cell line}}{IC_{50} \text{ of a compound toward cancer cell line}}$$

Results and discussion

Formulation of trimetallic free and loaded nanocomposites

Formulation of the trimetallic nanoparticles into the nanocomposite was carried out *via* a green method in which the cross linker and stabilizing and capping agents assisted in reducing the size of the biopolymers to the nanosize range. The CuNPs supported the stability of CrNPs and CoNPs.

Physicochemical analysis

The study of functional groups before and before composition was done using FTIR spectroscopy, as illustrated in Fig. 1. The five regions were targeted to understand the effect of composition. The first region 3500–3100 cm^{-1} presented the hydroxyl group and amino group stretching vibration of GLN at 3439 and 3855 cm^{-1}, respectively. HEC hydroxyl groups were assigned at 3419 cm^{-1} as a short-intensity band. The effect of composition was recorded in the Fcomp sample, where the OH band was

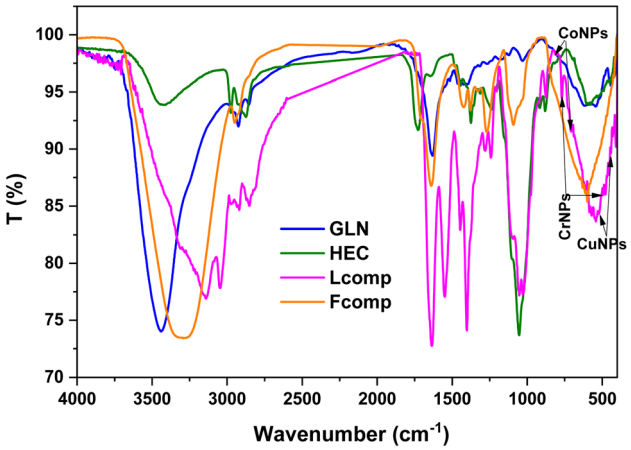

Fig. 1 FTIR spectra of the free and loaded nanocomposites and their neat materials.

observed at 3296 cm^{-1} with a high shift to low frequency with obvious broadness. Moreover, the loading of trimetallic nanoparticles reflected a high shifting of hydroxyl groups to low frequency (3146 cm^{-1}). The above observations affirmed a significant effect of neat materials after composition as well as after the loading of trimetallic nanoparticles. The region of CH stretching vibration (2990–2785 cm^{-1}) was presented as bands at 2922 and 2849 cm^{-1} (GLN), 2974 and 2874 cm^{-1} (HEC), 2970, 2919 and 2850 cm^{-1} (Fcomp) and 2947 cm^{-1} (Lcomp), which reflect the interaction of GLN and HEC molecules in Fcomp and the electron withdrawing interaction of trimetallic nanoparticles in Lcomp. The third region (1747–1219 cm^{-1}) of the ethyl groups vibration in HEC was not significantly affected.[37] Additionally, the amide I group band in GLN (1517 cm^{-1}) was shifted in Lcomp to 1550 cm^{-1}.[38] The region of C–O–C (1180–930 cm^{-1}) presented the bands at 1027, 1054, 1095, 1054 and 1025 for GLN, HEC, Fcomp and Lcomp, respectively. These results emphasized that the composition of neat materials does not affect the C–O_C group while the loading of trimetallic nanoparticles was significantly effective. The last region presented obvious bands at 522 and 438 cm^{-1} related to CuNPs[39] as well as bands at 814 and 578 cm^{-1} for M-O cobalt nanoparticles, respectively,[40,41] while CrNPs bands were observed at 767 and 498 cm^{-1}.[42] Hence, the FTIR findings confirmed the formulation of nanocomposites in both free and loaded forms.

The XRD patterns of GLN, HEC, Fcomp, and Lcomp are presented in Fig. 2. GLN and HEC showed an amorphous monotonous behavior with peaks at $2\theta = 17°$ (ref. 43) and 20°.[44,45] In addition, Fcomp presented one peak at $2\theta = 22°$ with a kind of sharpness that could be due to the crystalline structure obtained from the nanoformulation. Moreover, the Lcomp pattern illustrated the new structure after the loading of trimetallic nanoparticles, where the biopolymers region was observed at a small peak at $2\theta = 15°$, which was less sharp in comparison with that of Fcomp at 20°. However, the trimetallic components were observed at $2\theta = 30°$ and 33°, which could be the result of the overlap of CuNPs and CrNPs.[46,47] The peaks at $2\theta = 39°$ are related to CuNPs and CoNPs overlapping. The

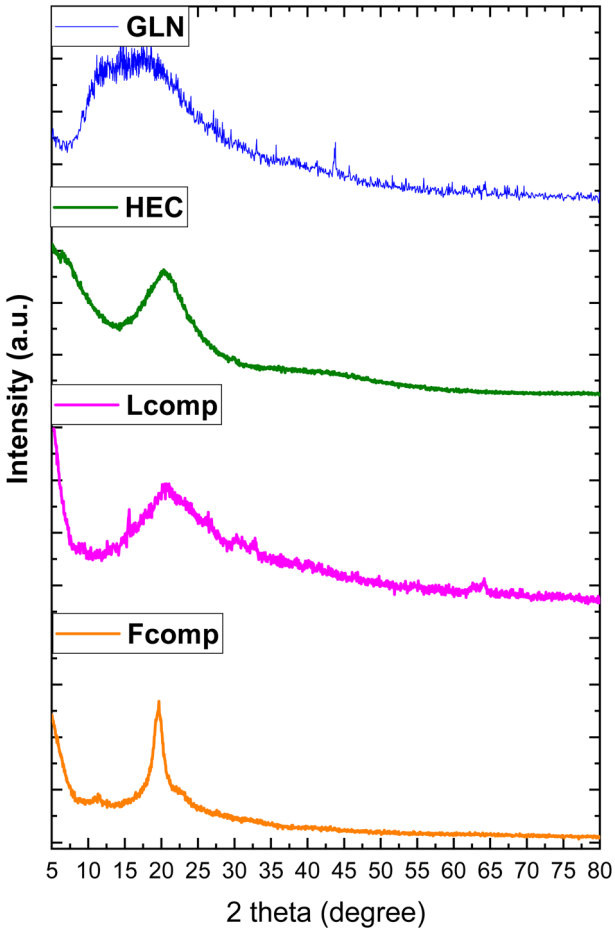

Fig. 2 XRD patterns of free and loaded nanocomposites and their neat materials.

peaks at $2\theta = 46°$ and 77° are related to the overlap of CuNPs, CrNPs, and CoNPs.[48] Consequently, CuNPs, CrNPs, and CoNPs were observed individually at $2\theta = 69°$,[47] 59°,[46] and 43°,[48] respectively. The crystal planes of the metals were compared to the reference cards for Cu (card no. 04-012-7238),[47] Cr (card no. 73-2134 23)[49] and Co (card no. 73-2134 23).[50] Finally, the XRD pattern findings emphasized the research hypothesis and confirmed the interaction of the nanocomposite components.

DLS

The DLS data tabulated in Table 1 includes the average zeta potential in mV, particle size in nm and polydispersity index (PDI). Fcomp showed a good average zeta potential of about −36 mV, which indicated excellent stability.[51] On the other side, Lcomp revealed about −24 mV, which is less than that of Fcomp

Table 1 DLS measurements of free and loaded nanocomposites

Nanocomposites	Av. zeta potential, mV	PDI	Average particle size/nm
Fcomp	−36 ± 3	0.4	169 ± 9
Lcomp	−24 ± 3	0.3	102 ± 6

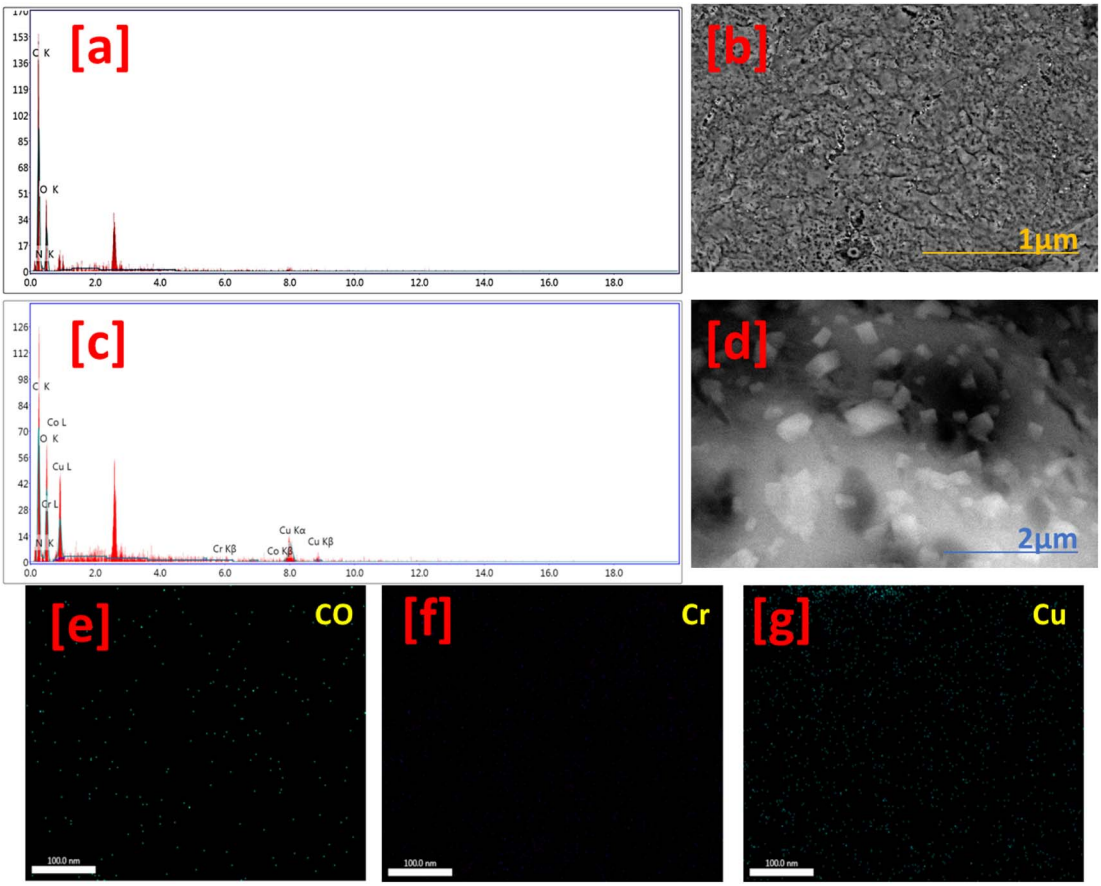

Fig. 3 SEM images and EDX results of the free composite (EDX (a) and SEM (b)) and loaded nanocomposite (EDX (c) and SEM (d)) and the elemental mapping of the loaded nanocomposite for Co (e), Cr (f), and Cu (g).

according to the dual phases and also confirmed the good stability. In addition, the particle size for Fcomp and Lcomp was 169 and 102 nm, respectively. On the other hand, the PDI of Fcomp was observed to be less than that of Lcomp, which may be because the trimetallic nanoparticles have good homogeneity and Lcomp has decreased surface charge, according to the interaction between the formulated nanoparticles and the biopolymers' active components.

Fig. 3 shows the topographical and EDX analysis of Fcomp and Lcomp. The Fcomp surface texture showed a porous and rough appearance with many wrinkles (Fig. 3b). Meanwhile, the Lcomp surface was similar to that of Fcomp surface, which was filled up with nanoparticles (Fig. 3c). Moreover, many crystals are homogeneously distributed on Lcomp (Fig. 3d). These crystals are clusters of aggregated trimetallic nanoparticles, according to the SEM results. On the other hand, the EDX results showed carbon, oxygen, and nitrogen atoms in the

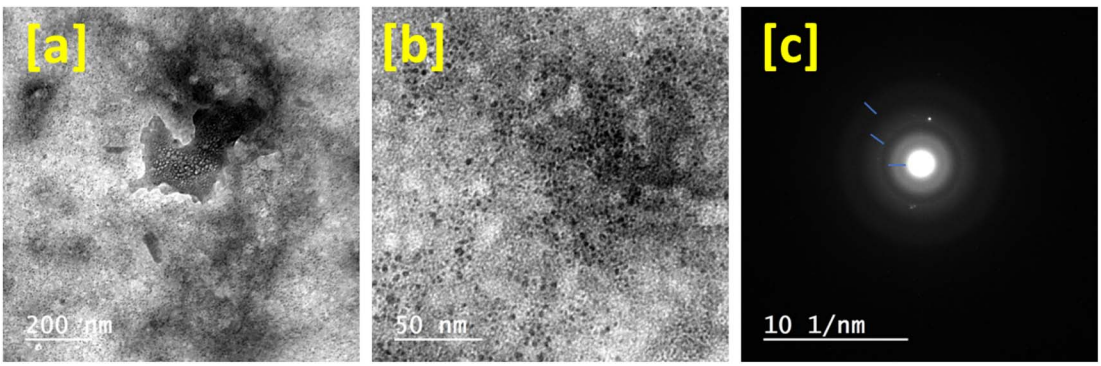

Fig. 4 TEM images of the loaded nanocomposite at low (a) and high (b) magnification, and the SAED pattern (c).

Fcomp sample (Fig. 3a). The Lcomp sample elemental composition was the same as that of Fcomp, in addition to copper, cobalt and chromium (Fig. 3c). Furthermore, elemental mapping images of Co ions (Fig. 3e) show a good distribution, similar to that of Cr ions (Fig. 3f) but with a lower amount in comparison with Cu (Fig. 3g), which was observed in a higher amount in comparison with Cr and Co elements. This could be related to the molecular weight of the elements. These observations are in a good agreement with the XRD findings.

The low and high magnification TEM images for Lcomp are presented in Fig. 4 with the SAED pattern. The low magnification image (Fig. 4a) shows the molecular structure of Lcomp, which presents nano-sized matrix biopolymers and trimetallic nanoparticles with size of about 113 nm. The high magnification image (Fig. 4b) illustrates the trimetallic nanoparticles with size of about 13 nm. Additionally, the SAED pattern (Fig. 4c) presents three circles with two polar positional points as a mirror and image. The polycrystalline behavior of Lcomp was affirmed by the ring diffractogram. Moreover, the polar spots could be related to the metal crystallinity as well.[52] These could be according to the dual phase composition of Lcomp and is in a good agreement with the DLS measurements.

Antimicrobial activity

Metal nanoparticles have gained significant attention as antimicrobial agents due to their unique physicochemical properties and broad-spectrum antimicrobial activity.[53] Recently, trimetallic nanoparticles composed of three different metals have received much attention due to their antimicrobial properties. While research on trimetallic nanoparticles as antimicrobial agents is relatively limited compared to monometallic nanoparticles, in this study, a nanocomposite based on trimetallic Cr–Co-CuNPs was synthesized. The synthesized Cu–Cr–Co-NPs@GLN-HEC nanocomposite and GLN-HEC were evaluated for antimicrobial activity, as illustrated in Fig. 5. Results showed that the synthesized Cu–Cr–Co-NPs@GLN-HEC nanocomposite exhibited antimicrobial activity toward the tested bacterial and fungal strains. Fig. 5 shows that the synthesized nanocomposite had outstanding antibacterial activity against *S. typhimurium*, *P. aeruginosa*, *S. aureus* and *S. mutans* with inhibition zones of 16, 17, 14 and 31 mm, respectively. Furthermore, the MIC of the CuNPs@GLN-HEC nanocomposite toward all bacterial strains was performed, whose results illustrated that the MICs of the CuNPs@GLN-HEC nanocomposite toward *S. typhimurium*, *P. aeruginosa*, *S. aureus* and *S. mutans* were 125, 62.5, 125 and 7.81 μg mL^{-1}, respectively (Table 2). From these data, the bacterial strain most affected by the synthesized CuNPs@GLN-HEC nanocomposite is *S. mutans*, while least sensitive bacterial strains are *S. typhimurium* and *S. aureus*.

The synthesized CuNPs@GLN-HEC nanocomposite also showed antifungal activity against *C. albicans* and *C. neoformans*, as shown in Fig. 5. Results showed that the synthesized CuNPs@GLN-HEC nanocomposite showed antifungal activity toward *C. albicans* and *C. neoformans* with inhibition zones of 16 and 19 mm, respectively. Furthermore, the MICs of the CuNPs@GLN-HEC nanocomposite toward both the strains were 31.25 and 15.62 μg mL^{-1}, respectively, where *C. neoformans* was

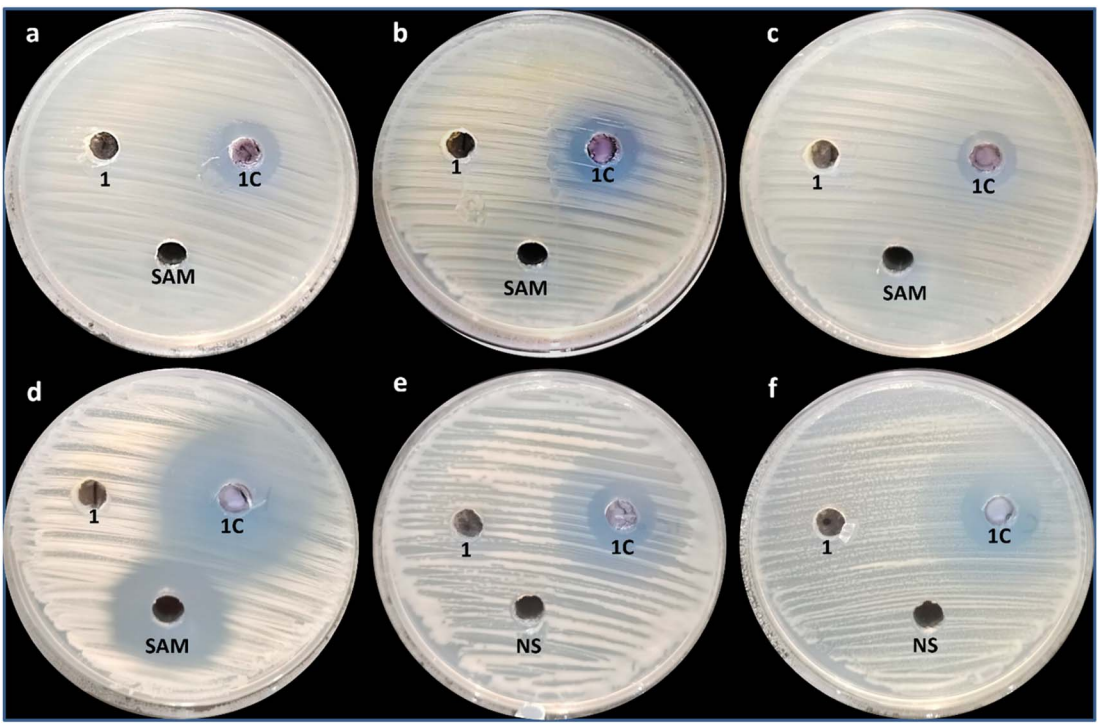

Fig. 5 Antimicrobial activity of the Cu–Cr–Co-NPs@GLN-HEC nanocomposite (1C), GLN-HEC (1) and SAM/NS toward *S. typhimurium* (a), *P. aeruginosa* (b), *S. aureus* (c), *S. mutans* (d), *C. albicans* (e) and *C. neoformans* (f) using the agar-well diffusion method.

Table 2 Minimum inhibitory concentrations of the Cu–Cr–Co-NPs@GLN-HEC nanocomposite toward all the tested strains

	MIC (μg mL^{-1})
Microbial strain	Cu–Cr–Co-NPs@GLN-HEC
S. typhimurium	125
P. aeruginosa	62.5
S. aureus	125
S. mutans	7.81
C. albicans	31.25
C. neoformans	15.62

more sensitive to C1 than *C. albicans*. Hashem, Al-Askar[54] successfully conducted the mycosynthesis of trimetallic copper oxide–selenium–zinc oxide nanoparticles. These nanoparticles demonstrated antifungal properties against fungi that cause mucormycosis, with minimum inhibitory concentrations (MICs) ranging from 1.95 to 62.5 μg mL^{-1}. Cu/Cr/Ni trimetallic oxide nanoparticles were synthesised using aqueous leaf extracts of *Eryngium campestre* and *Froriepia subpinnata*. The antimicrobial activity of these nanoparticles was evaluated, and the results demonstrated that they exhibited antibacterial effects against *E. coli* and *S. aureus*.[55] utilised garlic leaf to create a ruthenium/silver/palladium trimetallic nanocomposite (Ru/Ag/Pd)-Np. The antimicrobial findings verified that this nanocomposite displayed antibacterial effects against *E. coli* and *B. cereus* as well as antifungal properties against *Aspergillus flavus*, *Aspergillus niger*, *Candida albicans*, and *C. glabrata*.

The antimicrobial mechanisms of trimetallic Cr–Co–Cu nanoparticles can be attributed to the individual antimicrobial properties of each metal component as well as the potential synergistic effects arising from their combination. Trimetallic nanoparticles containing chromium (Cr), cobalt (Co), and copper (Cu) can exhibit antimicrobial effects through various mechanisms. These metal nanoparticles can release metal ions, which have been shown to induce oxidative stress and damage microbial cells. Metal ions can disrupt cell membranes, inhibit enzyme activity, and interfere with the DNA replication and protein synthesis of microorganisms, leading to their growth inhibition or death.[53,56]

Evaluation of the cytotoxicity of Cu–Cr–Co-NPs@GLN-HEC and GLN-HEC on the normal cell line

As an essential component of preclinical research, assessing the cytotoxicity of compounds on normal cell lines requires the determination of a compound's potential toxicity to healthy cells.[57] In this regard, determining the biosafety of compounds is regarded as the initial step toward their implementation in various disciplines. In the current study, the cytotoxicity of Cu–Cr–Co-NPs@GLN-HEC and GLN-HEC was assessed toward Wi38 normal cell line, as illustrated in Fig. 6. Results showed that the IC_{50} of the Cu–Cr–Co-NPs@GLN-HEC nanocomposite toward the Wi38 cell line was 170.8 μg mL^{-1}, and the cell viability of Cu–Cr–Co-NPs@GLN-HEC at concentrations of 31.25, 62.5 and 125 μg mL^{-1} was 99.3, 88.49 and 61.8%, respectively. In general, if the IC_{50} is ≥ 90 μg mL^{-1}, the material is classified as non-cytotoxic.[58] Therefore, the synthesized Cu–Cr–Co-NPs@GLN-HEC nanocomposite is considered safe to use. Thus, safe concentrations and maximum non-toxic concentrations of this nanocomposite were checked for anticancer activity.

Anticancer activity of Cu–Cr–Co-NPs@GLN-HEC and GLN-HEC

The synthesis of anticancer compounds is critical because it facilitates the identification and advancement of novel pharmaceuticals, which may result in significant advances in the treatment of cancer.[59] By synthesizing and modifying compounds, researchers can establish the structure–activity relationship, optimize drug properties, and overcome drug resistance, providing alternative options for patients.[60] In this study, the anticancer activity of the synthesized Cu–Cr–Co-NPs@GLN-HEC nanocomposite and its start materials were evaluated toward the MCF7 cancerous cell line, as shown in Fig. 7. Results illustrated that the IC_{50} of the Cu–Cr–Co-NPs@GLN-HEC nanocomposite was 30.4 μg mL^{-1}, which confirms that this nanocomposite has promising anticancer activity. Moreover, the anticancer activity of Cu–Cr–Co-NPs@GLN-HEC at safe concentrations of 125, 62.5 and 31.25

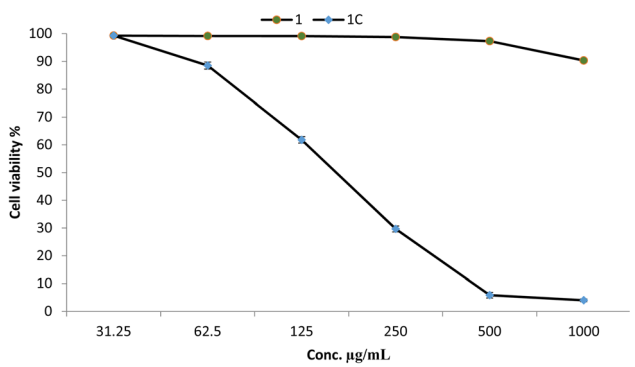

Fig. 6 Cytotoxicity of Cu–Cr–Co-NPs@GLN-HEC (1C) and GLN-HEC (1) at different concentrations against the Wi38 normal cell line.

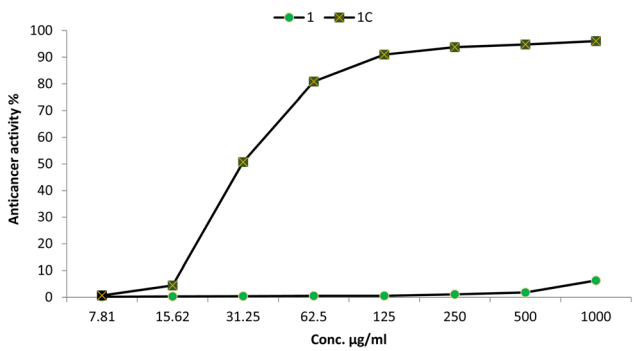

Fig. 7 Anticancer activity of Cu–Cr–Co-NPs@GLN-HEC (1C) and GLN-HEC (1) against the MCf7 cell line.

were 90.9, 80.83 and 50.69%, respectively. Also, the SI was calculated for the nanocomposite, where it was 5.61. This result confirms that the synthesized Cu–Cr–Co-NPs@GLN-HEC nanocomposite is safe for use because the compounds possessing SI values greater than two are considered to have acceptable selectivity toward cancer cells.[61]

Nanometals have received much attention due to their high efficacy as antimicrobial as well as anticancer agents.[62–64] Khan *et al.*[65] reported that cobalt oxide nanoparticles exhibited promising anticancer activity toward the colorectal cancerous cell line HT29, where the IC_{50} was 2.26 μg mL^{-1}. Moreover, cobalt oxide nanoparticles, which were functionalized by glutamic acid and conjugated with thiosemicarbazide, showed anticancer activity against the gastric cancer (AGS) cell line with IC_{50} = 107.5 μg mL^{-1}.[66] Likewise, chromium oxide nanoparticles displayed promising anticancer activity toward the MCF7 cancerous cell line.[67] Also, Adnan and Mohammed[68] confirmed that chromium oxide nanoparticles have outstanding anticancer activity against the A549 cancerous cell line where the cytotoxicity was greater than 70% at concentrations of 6.25–100 μg mL^{-1}. Additionally,[69] reported that the nanocomposite based on mycosynthesized nanoparticles with starch displayed anticancer activity toward the MCF7 cancerous cell line where the IC_{50} was 62.8 μg mL^{-1}.

Trimetallic nanoparticles have recently become a subject of great interest in the field of anticancer research because of their distinct characteristics and potential use in therapy.[70] conducted the production of trimetallic nanoparticles consisting of gold (Au), platinum (Pt), and silver (Ag) using *Pleurotus florida*. These nanoparticles exhibited a spherical morphology and varied in size, ranging from 4 to 10 nm. Trimetallic nanoparticles were synthesized and evaluated against the mda-mb-231 triple negative breast cancer cell line. The maximum cell viability, reaching 10%, was seen at a nanoparticle concentration of 100 μg mL^{-1}. According to a report by Hussein *et al.*[71] the synthesized trimetallic Ru/Ag/Pd nanoparticles exhibited anti-cancer properties against the HepG2, Caco-2, and K562 cell lines.[66] conducted a study where they produced silver–cobalt–ferrite nanoparticles utilizing *Citrus limon*. These nanoparticles were found to possess anticancer properties against HEPG2 and MCF7 cell lines, with an IC_{50} value of 43.5 and 35.5 μg mL^{-1}, respectively.

Nanocomposites based on trimetallic nanoparticles, gelatin, and hydroxyethyl cellulose can exhibit several anticancer mechanisms. The nanocomposite structure allows for the encapsulation or conjugation of anticancer drugs within the gelatin and hydroxyethyl cellulose matrix. This enables controlled and targeted drug delivery to the cancer cells.[72] The trimetallic nanoparticles incorporated into the nanocomposite can further enhance drug delivery by facilitating cellular uptake and improving drug release kinetics, leading to increased drug concentration at the tumor site.[73] Trimetallic nanoparticles within the nanocomposite can exhibit inherent anticancer properties.[74] The combination of different metals, such as cobalt, chromium, and copper, can induce synergistic effects, resulting in enhanced cytotoxicity against cancer cells. The nanoparticles can interact with cellular components, disrupt cellular processes, and induce cell death through various mechanisms, including oxidative stress, DNA damage, and apoptosis.[75]

Conclusion

This study successfully synthesized a novel trimetallic nanocomposite (Cu–Cr–Co-NPs@GLN-HEC) by integrating copper, cobalt, chromium, gelatin, and hydroxyethyl cellulose. The nanocomposite's structure and dimensions were thoroughly characterized using a range of techniques, confirming its formation as trimetallic nanoparticles with sizes ranging from 102 nm to 169 nm. These findings demonstrate the successful fabrication of a novel nanocomposite with controlled size and composition. The synthesized Cu–Cr–Co-NPs@GLN-HEC nanocomposite displayed remarkable antimicrobial properties against a diverse range of bacteria and fungi. The nanocomposite exhibited potent antibacterial activity against *S. typhimurium*, *P. aeruginosa*, *S. aureus*, and *S. mutans*, with MICs ranging from 7.81 to 125 μg mL^{-1}. Additionally, the nanocomposite demonstrated promising antifungal activity against C. albicans and C. neoformans, with MICs of 15.62 and 31.25 μg mL^{-1}, respectively. These results highlight the potential of this nanocomposite for combating a broad spectrum of microbial infections. Furthermore, the study explored the anticancer potential of the synthesized nanocomposite. Cu–Cr–Co-NPs@GLN-HEC exhibited strong anticancer activity against MCF7 breast cancer cells, with an IC50 value of 30.4 μg mL^{-1}. Importantly, the nanocomposite demonstrated relatively low cytotoxicity against normal Wi38 cells, suggesting a promising therapeutic window for cancer treatment. The observed anticancer activity, coupled with the nanocomposite's antimicrobial properties, positions it as a promising candidate for future development in the medical field. Although the elaborated hybrid system based on three metal nanoparticles and sustainable polymers brought about considerable performance and properties, the surface and bulk engineering of such sustainable structures with bimetallic or trimetallic supports and other biopolymers may result in a wider spectrum of possibilities in antibacterial and anticancer activities, which can be a topic for future investigations.

Data availability

The data and materials are available as per request.

Author contributions

Mohamed S. Hasanin: conceptualization, methodology, writing – original draft preparation, writing – review and editing; Mostafa A. Abdel-Maksoud: methodology, writing – original draft preparation; Mohamed A. El-Tayeb: writing – review and editing, critically revising; Bushra Hafeez Kiani: writing – review and editing, critically revising, Amr H. Hashem: conceptualization, methodology, writing – original draft preparation, writing – review and editing.

Conflicts of interest

The authors declare that they have no conflict of interests.

Acknowledgements

The authors would like to thank Botany and Microbiology Department, Faculty of Science, Al-Azhar University, and National Research Centre, Dokki, Giza for promoting this research. The authors extend their appreciation to the Researchers Supporting Project number (RSPD2024R678) King Saud University, Riyadh, Saud Arabia.

References

1 M. Abolhasani and E. Kumacheva, The rise of self-driving labs in chemical and materials sciences, *Nat., Synth.*, 2023, **2**(6), 483–492.
2 R. M. Abdelhameed and M. S. Hasanin, The potential of MOFs embedded in banana cellulose materials for application in dialysis, *J. Mol. Liq.*, 2024, 124931.
3 M. S. Hasanin, *et al.*, New Eco-Friendly, Biocompatible, Bactericidal, Fungicidal and Anticancer-Activity-Exhibiting Nanocomposites Based on Bimetallic TiO2@ Cr2O3 Nanoparticle Core and Biopolymer Shells, *J. Compos. Sci.*, 2023, **7**(10), 426.
4 S. R. Singh, N. Krishnamurthy and B. B. Mathew, A review on recent diseases caused by microbes, *J. Appl. Environ. Microbiol.*, 2014, **2**(4), 106–115.
5 M. Malone and G. Schultz, Challenges in the diagnosis and management of wound infection, *Br. J. Dermatol.*, 2022, **187**(2), 159–166.
6 A. P. Rogers, S. J. Mileto and D. Lyras, Impact of enteric bacterial infections at and beyond the epithelial barrier, *Nat. Rev. Microbiol.*, 2023, **21**(4), 260–274.
7 G. Garber, An overview of fungal infections, *Drugs*, 2001, **61**, 1–12.
8 N. M. Aljamali, Z. H. Al-zubaidy and A. H. Enad, Bacterial infection and common bacterial diseases: A Review, *Pharm. Nanotechnol.*, 2021, **3**, 13–23.
9 M. A. Salam, *et al.*, Antimicrobial resistance: a growing serious threat for global public health, *Healthcare*, 2023, **11**(13), 1946.
10 M. A. Abushaheen, *et al.*, Antimicrobial resistance, mechanisms and its clinical significance, *Disease-a-Month*, 2020, **66**(6), 100971.
11 S. Fletcher, Understanding the contribution of environmental factors in the spread of antimicrobial resistance, *Environ. Health Prev. Med.*, 2015, **20**, 243–252.
12 M. A. A. Majumder, *et al.*, Antimicrobial stewardship: Fighting antimicrobial resistance and protecting global public health, *Infect. Drug Resist.*, 2020, 4713–4738.
13 B. Koul and B. Koul, *Types of Cancer. Herbs for Cancer Treatment*, 2019, pp. 53–150.
14 S. J. Nass, *et al.*, *Guiding cancer control: A path to transformation*, 2019.
15 E. Liebermann, *et al.*, Roles and activities of nurses in prevention and early detection of cancer in low-and middle-income countries: a scoping review, *Asia Pac. J. Oncol. Nurs.*, 2023, 100242.
16 T. Byers, *et al.*, American Cancer Society guidelines on nutrition and physical activity for cancer prevention: reducing the risk of cancer with healthy food choices and physical activity, *Ca-Cancer J. Clin.*, 2002, **52**(2), 92–119.
17 B. S. Chhikara and K. Parang, Global Cancer Statistics 2022: the trends projection analysis, *Chem. Biol. Lett.*, 2023, **10**(1), 451.
18 Y. Zhao, F. Liu and W. Wang, Treatment progress of spinal metastatic cancer: a powerful tool for improving the quality of life of the patients, *J. Orthop. Surg. Res.*, 2023, **18**(1), 563.
19 S. Ibrahim, H. Elsayed and M. Hasanin, Biodegradable, antimicrobial and antioxidant biofilm for active packaging based on extracted gelatin and lignocelluloses biowastes, *J. Polym. Environ.*, 2021, **29**, 472–482.
20 M. Hasanin, *et al.*, Green decoration of graphene oxide Nano sheets with gelatin and gum Arabic for targeted delivery of doxorubicin, *Biotechnol. Rep.*, 2022, **34**, e00722.
21 S. Selvaraj, *et al.*, A state-of-the-art review on plant-derived cellulose-based green hydrogels and their multifunctional role in advanced biomedical applications, *Int. J. Biol. Macromol.*, 2024, 130991.
22 G. F. El Fawal, *et al.*, Hydroxyethyl cellulose hydrogel for wound dressing: Fabrication, characterization and in vitro evaluation, *Int. J. Biol. Macromol.*, 2018, **111**, 649–659.
23 E. Sánchez-López, *et al.*, Metal-based nanoparticles as antimicrobial agents: an overview, *Nanomaterials*, 2020, **10**(2), 292.
24 H. Lei, *et al.*, Recent progress of metal-based nanomaterials with anti-tumor biological effects for enhanced cancer therapy, *Exploration*, 2023, **3**(5), 20220001.
25 B. A. Aderibigbe, Metal-based nanoparticles for the treatment of infectious diseases, *Molecules*, 2017, **22**(8), 1370.
26 M. M. Abdel-Kareem and A. Zohri, Extracellular mycosynthesis of gold nanoparticles using Trichoderma hamatum: optimization, characterization and antimicrobial activity, *Lett. Appl. Microbiol.*, 2018, **67**(5), 465–475.
27 E. Darvishi, D. Kahrizi and E. Arkan, Comparison of different properties of zinc oxide nanoparticles synthesized by the green (using Juglans regia L. leaf extract) and chemical methods, *J. Mol. Liq.*, 2019, **286**, 110831.
28 H.-J. Yen, *et al.*, Toxic effects of silver and copper nanoparticles on lateral-line hair cells of zebrafish embryos, *Aquat. Toxicol.*, 2019, **215**, 105273.
29 P. Abhimanyu, M. Arvind and N. Kishor, Biosynthesis of CuO Nanoparticles Using Plant Extract as a Precursor: Characterization, Antibacterial, and Antioxidant Activity, *Nano Biomed. Eng.*, 2023, **15**(4), 369.
30 S. M. Ansari, *et al.*, Cobalt nanoparticles for biomedical applications: Facile synthesis, physiochemical

characterization, cytotoxicity behavior and biocompatibility, *Appl. Surf. Sci.*, 2017, **414**, 171–187.
31 S. Chandra and A. Kumar, Spectral, thermal and morphological studies of chromium nanoparticles, *Spectrochim. Acta, Part A*, 2013, **102**, 250–255.
32 Standards, N.C.f.C.L., *Reference Method for Broth Dilution Antifungal Susceptibility Testing of Yeasts*, National Committee for Clinical Laboratory Standards Wayne, PA, 2002.
33 C. Valgas, *et al.*, Screening methods to determine antibacterial activity of natural products, *Braz. J. Microbiol.*, 2007, **38**, 369–380.
34 A. H. Hashem, *et al.*, Biomedical Applications of Mycosynthesized Selenium Nanoparticles Using Penicillium expansum ATTC 36200, *Biol. Trace Elem. Res.*, 2021, **199**, 3998–4008.
35 S. Dacrory, A. H. Hashem and M. Hasanin, Synthesis of cellulose based amino acid functionalized nano-biocomplex: Characterization, antifungal activity, molecular docking and hemocompatibility, *Environ. Nanotechnol. Monit. Manag.*, 2021, **15**, 100453.
36 A. Van de Loosdrecht, *et al.*, A tetrazolium-based colorimetric MTT assay to quantitate human monocyte mediated cytotoxicity against leukemic cells from cell lines and patients with acute myeloid leukemia, *J. Immunol. Methods*, 1994, **174**(1–2), 311–320.
37 F. Şen and M. V. Kahraman, Preparation and characterization of hybrid cationic hydroxyethyl cellulose/sodium alginate polyelectrolyte antimicrobial films, *Polym. Adv. Technol.*, 2018, **29**(7), 1895–1901.
38 M. Qadir, *et al.*, Preparation and characterization of gelatin-hydroxyapatite composite for bone tissue engineering, *Int. J. Eng. Technol. Sci.*, 2014, **14**, 24.
39 M. Elango, *et al.*, Synthesis, Characterization, and Antibacterial Activity of Polyindole/Ag–Cuo Nanocomposites by Reflux Condensation Method, *Polym.-Plast. Technol. Eng.*, 2018, **57**(14), 1440–1451.
40 G. Allaedini and A. Muhammad, Study of influential factors in synthesis and characterization of cobalt oxide nanoparticles, *J. Nanostruct. Chem.*, 2013, **3**, 1–16.
41 M. Hafeez, *et al.*, Green synthesis of cobalt oxide nanoparticles for potential biological applications, *Mater. Res. Express*, 2020, **7**(2), 025019.
42 M. K. Trivedi, *et al.*, Characterization of physical, thermal and structural properties of chromium (VI) oxide powder: Impact of biofield treatment, *J. Powder Metall. Min.*, 2015, **4**(1), 1000128.
43 H.-A. S. Tohamy, *et al.*, Preparation of hydroxyethyl cellulose/mangiferin edible films and their antimicrobial properties, *BMC Chem.*, 2022, **16**(1), 113.
44 L. Radev, *et al.*, Organic/Inorganic bioactive materials Part III: in vitro bioactivity of gelatin/silicocarnotite hybrids, *Open Chem.*, 2009, **7**(4), 721–730.
45 M. P. Das, *et al.*, Extraction and characterization of gelatin: a functional biopolymer, *Int. J. Pharm. Pharmaceut. Sci.*, 2017, **9**(9), 239–242.
46 T. Satgurunathan, P. S. Bhavan and R. D. S. Joy, Green Synthesis of Chromium Nanoparticles and Their Effects on the Growth of the Prawn Macrobrachium rosenbergii Post-larvae, *Biol. Trace Elem. Res.*, 2019, **187**(2), 543–552.
47 T. Liyuan, *et al.*, Green synthesised CuNPs using Alhagi maurorum extract and its ability to amelioration of Mycoplasma pneumoniae infected pneumonia mice model, *J. Exp. Nanosci.*, 2022, **17**(1), 585–598.
48 M. S. Hodhod, *et al.*, Green synthesis, characterization, and evaluation of antibacterial activities of cobalt nanoparticles produced by marine fungal species Periconia prolifica, *Open Chem.*, 2023, **21**(1), 20230139.
49 P. Gibot, Centimetric-sized chromium (III) oxide object synthesized by means of the carbon template replication, *Ceramics*, 2020, **3**(1), 92–100.
50 M. Salavati-Niasari, A. Khansari and F. Davar, Synthesis and characterization of cobalt oxide nanoparticles by thermal treatment process, *Inorg. Chim. Acta*, 2009, **362**(14), 4937–4942.
51 G. Midekessa, *et al.*, Zeta potential of extracellular vesicles: toward understanding the attributes that determine colloidal stability, *ACS Omega*, 2020, **5**(27), 16701–16710.
52 M. De Graef, *Introduction to Conventional Transmission Electron Microscopy*, Cambridge University Press, Cambridge, 2003.
53 K. Skłodowski, Metallic Nanosystems in the Development of Antimicrobial Strategies with High Antimicrobial Activity and HighBiocompatibility, *Int. J. Mol. Sci.*, 2023, **24**(3), 2104.
54 A. H. Hashem, *et al.*, Biosynthesis, Characterization, and Antifungal Activity of Novel Trimetallic Copper Oxide–Selenium–Zinc Oxide Nanoparticles against Some Mucorales Fungi, *Microorganisms*, 2023, **11**(6), 1380.
55 Z. Vaseghi, O. Tavakoli and A. Nematollahzadeh, Rapid biosynthesis of novel Cu/Cr/Ni trimetallic oxide nanoparticles with antimicrobial activity, *J. Environ. Chem. Eng.*, 2018, **6**(2), 1898–1911.
56 M. H. Mujahid, *et al.*, Metallic and metal oxide-derived nanohybrid as a tool for biomedical applications, *Biomed. Pharmacother.*, 2022, **155**, 113791.
57 C. E. Gîrd, T. Costea and V. Mitran, Evaluation of cytotoxic activity and anticancer potential of indigenous Rosemary (Rosmarinus officinalis L.) and Oregano (Origanum vulgare L.) dry extracts on MG-63 bone osteosarcoma human cell line, *Rom. J. Morphol. Embryol.*, 2021, **62**(2), 525–535.
58 J.-R. Ioset, *et al.*, *Drug Screening for Kinetoplastids Diseases. A Training Manual for Screening in Neglected Diseases*, 2009.
59 P. Chunarkar-Patil and M. Kaleem, Anticancer Drug Discovery Based on Natural Products: From Computational Approaches to Clinical Studies, *Biomedicines*, 2024, **12**(1), 201.
60 T. Hu, Nanomedicines for Overcoming Cancer Drug Resistance, *Pharmaceutics*, 2022, **14**(8), 1606.
61 T. Nasr, *et al.*, Synthesis, antitumor evaluation and microarray study of some new pyrazolo [3, 4-d][1, 2, 3] triazine derivatives, *Eur. J. Med. Chem.*, 2017, **141**, 603–614.

62 O. M. Ali, *et al.*, Green biosynthesis of titanium dioxide quantum dots using watermelon peel waste: Antimicrobial, antioxidant, and anticancer activities, *Biomass Convers. Biorefin.*, 2024, **14**(5), 6987–6998.
63 E. Saied, *et al.*, Photocatalytic and antimicrobial activities of biosynthesized silver nanoparticles using Cytobacillus firmus, *Life*, 2022, **12**(9), 1331.
64 A. H. Hashem and G. S. El-Sayyad, Antimicrobial and anticancer activities of biosynthesized bimetallic silver-zinc oxide nanoparticles (Ag-ZnO NPs) using pomegranate peel extract, *Biomass Convers. Biorefin.*, 2023, 1–13.
65 S. Khan, *et al.*, In vitro evaluation of anticancer and antibacterial activities of cobalt oxide nanoparticles, *JBIC, J. Biol. Inorg. Chem.*, 2015, **20**(8), 1319–1326.
66 M. Jarestan, *et al.*, Preparation, characterization, and anticancer efficacy of novel cobalt oxide nanoparticles conjugated with thiosemicarbazide, *3 Biotech*, 2020, **10**(5), 230.
67 S. A. Khan, *et al.*, Green Synthesis of Chromium Oxide Nanoparticles for Antibacterial, Antioxidant Anticancer, and Biocompatibility Activities, *Int. J. Mol. Sci.*, 2021, **22**(2), 502.
68 W. G. Adnan and A. M. Mohammed, Green synthesis of chromium oxide nanoparticles for anticancer, antioxidant and antibacterial activities, *Inorg. Chem. Commun.*, 2024, **159**, 111683.
69 M. Hasanin, *et al.*, Ecofriendly Synthesis of Biosynthesized Copper Nanoparticles with Starch-Based Nanocomposite: Antimicrobial, Antioxidant, and Anticancer Activities, *Biol. Trace Elem. Res.*, 2022, **200**(5), 2099–2112.
70 V. K. Chaturvedi, *et al.*, Rapid eco-friendly synthesis, characterization, and cytotoxic study of trimetallic stable nanomedicine: A potential material for biomedical applications, *Biochem. Biophys. Rep.*, 2020, **24**, 100812.
71 S. Hussein, *et al.*, Green synthesis of trimetallic nanocomposite (Ru/Ag/Pd)-Np and its in vitro antimicrobial and anticancer activities, *J. Chem.*, 2022, 1–14.
72 A. Mondal, A. K. Nayak and P. Chakraborty, Natural Polymeric Nanobiocomposites for Anti-Cancer Drug Delivery Therapeutics: A Recent Update, *Pharmaceutics*, 2023, **15**(8), 2064.
73 W. Zhang and R. Taheri-Ledari, Effects of morphology and size of nanoscale drug carriers on cellular uptake and internalization process: a review, *RSC Adv.*, 2023, **13**, 80–114.
74 M. Nasrollahzadeh and M. Sajjadi, Trimetallic Nanoparticles: Greener Synthesis and Their Applications, *Nanomaterials*, 2020, **10**(9), 1784.
75 U. Kim, *et al.*, Phloretin inhibits the human prostate cancer cells through the generation of reactive oxygen species, *Pathol. Oncol. Res.*, 2020, **26**, 977–984.